J. Phys. B: At. Mol. Opt. Phys. 28 (1995) 711–724. Printed in the UK

Charge transfer in slow N^{2+} + H collisions

B Herrero†, I L Cooper‡, A S Dickinson† and D R Flower§

† Department of Physics, The University of Newcastle upon Tyne, Newcastle upon Tyne NE1 7RU, UK

‡ Department of Chemistry, The University of Newcastle upon Tyne, Newcastle upon Tyne, NE1 7RU, UK

§ Department of Physics, The University of Durham, Durham, DH1 3LE, UK

Received 17 November 1994

Abstract. We have performed quantal calculations of charge transfer in N^{2+} + H collisions in the range of centre of mass energies $0.1 < E < 100$ eV amu^{-1}. Molecular states were calculated using *ab initio* SCF-CI methods. Radial and angular couplings between the adiabatic molecular states were evaluated with allowance for a common translation factor. In agreement with earlier calculations, we find that charge transfer into the $N^+(2s2p^3\ ^3D^o)$ state is dominant in the energy range considered and relevant to the study of photoionized nebulae. However, the cross sections and the rate coefficients that we have computed are smaller than the results of the earlier work by factors of about 1.5.

1. Introduction

The ions which are present in astrophysical plasmas can capture electrons in three ways: by radiative recombination, dielectronic recombination or through charge transfer with an atom. The last process does not involve a radiative step and can be intrinsically rapid, with a rate coefficient of order 10^{-9} cm^3 s^{-1} at temperatures $T \approx 10^4$ K. Electron capture occurs from the most abundant atoms in the plasma, H or He. Although the fraction of hydrogen in atomic form may be small, owing to ionization processes, its high elemental abundance ensures that it remains a major atomic species. Accordingly, the accurate determination of the distribution of heavy elements amongst their ionization stages requires a knowledge of the rate coefficients for electron capture from atomic hydrogen. Of those elements which are heavier than helium, the members of the CNO group have the largest cosmic abundances.

Nitrogen has been extensively observed in the spectra of gaseous nebulae. In particular, forbidden lines of N II occur in the visual part of the spectrum and have been observed for many years. The advent of the International Ultraviolet Explorer satellite enabled intercombination transitions of N III (and N IV) to be routinely observed. The interpretation of these observations involves a comparison with models of the ionization structure of the nebulae. Such models require atomic data relating to ionization and recombination processes, including charge transfer with atomic hydrogen.

In the present paper, we turn our attention to electron capture by N^{2+} from H, with both reactants initially in their ground states:

$$N^{2+}(1s^2 2s^2 2p\ ^2P^o) + H(1s) \longrightarrow N^+ + H^+ . \qquad (1)$$

0953-4075/95/040711+14$19.50

Previous work by Butler *et al* (1980) and Heil *et al* (1981) has shown this process to be rapid at the temperatures which prevail in nebulae. Heil *et al* (1981) considered the radial coupling between the two channels of $^3\Pi$ symmetry which dissociate either to the reactants above or to $N^+(2s2p^3\ ^3D^o) + H^+$. Wilkie *et al* (1985) subsequently made measurements of charge transfer in this system, using translational energy spectroscopy in the range of centre-of-mass energies between 43 and 570 eV amu^{-1}. At these energies mechanisms which are expected to be unimportant in the vicinity of 1 eV amu^{-1}, relevant to the nebulae, may contribute to the cross sections.

Using the molecular data of Heil *et al* (1981), Bienstock *et al* (1986) calculated additional values of the cross section for charge transfer into $N^+(2s2p^3\ ^3D^o)$ to compare with the state-selective measurements of Wilkie *et al* (1985). The calculated values exceeded the measurements, particularly at the higher energies. Bienstock *et al* also estimated, using the Landau–Zener model, the cross section for the production of $N^+(2s2p^3\ ^3P^o)$ associated with a distant avoided crossing, again in $^3\Pi$ symmetry, at a separation near 11 a_0. However their estimate of the energy at which the peak of the cross section occurred was well below 43 eV amu^{-1}, while the observations of Wilkie *et al* showed the cross section into $N^+(2s2p^3\ ^3P^o)$ generally increasing with energy up to about 570 eV amu^{-1}, the limit of their measurements.

With the major advances in computing power since the work of Heil *et al* (1981) it is possible to re-examine this problem, with the inclusion of additional channels in the triplet system and investigation of the singlet system. Alternative methods of calculating the non-adiabatic couplings other than that of the Hellmann–Feynman approximation used by Heil *et al* are now available (Cooper 1991). Also, while electron translation factors (Macias and Riera 1982, Kimura and Lane 1990) are not expected to play a major role at low velocities, it is now relatively straightforward to include them in quantal calculations of the nuclear motion (Gargaud *et al* 1987).

In section 2 we review the theoretical methods that are employed. In section 3 we describe the molecular calculations and, in section 4, we discuss the cross sections and rate coefficients obtained. Our conclusions are given in section 5.

2. Method

In the low velocity region considered in this work, the molecular expansion method (Kimura and Lane 1990) is appropriate. In this approach the electronic part of the wavefunction is represented by an expansion in terms of suitably chosen adiabatic molecular wavefunctions of the $(NH)^{2+}$ system. Transitions between these adiabatic states are induced by non-adiabatic couplings. At such low energies, a full quantal calculation is necessary to describe the nuclear motion correctly.

2.1. Molecular wavefunctions

Owing to the partially occupied s and p shells and the importance of core excitations and rearrangements, an *ab initio* calculation of the adiabatic energies and wavefunctions is required. As in previous work (Forster *et al* 1991), we have used the generalized atomic and molecular electronic structure system (GAMESS) (Guest *et al* 1993). Briefly, a self-consistent field unrestricted Hartree–Fock (SCF-UHF) calculation is first performed. The SCF orbitals are then introduced in a multi-reference determinant single- and double-excitation configuration-interaction (MRDCI) wavefunction, to determine energies and molecular wavefunctions for various symmetries over a range of internuclear separations.

Table 1. The nitrogen s-orbital basis. The contracted s-orbital. The nitrogen contracted s-orbital. Exponents for uncontracted nitrogen s-orbitals: 103.9936, 47.279 44, 22.218 71, 10 735 69, 5.3088 56 2.639 177, 1.165 764, 0.537 091, 0.244 904 and 0.110 271.

Exponents	Contraction coefficients
1 296 296	0.000 001
194 068.6	0.000 011
44 160.57	0.000 058
12 507.72	0.000 246
4 080.476	0.000 896
1 473.140	0.002 922
574.6066	0.008 689
238.3700	0.023 705

Table 2. The nitrogen p- and d-orbital basis. The eight nitrogen contracted p_x, p_y and p_z orbitals. Exponents for uncontracted nitrogen d orbitals: 3.2, 1.0, 0.3.

Exponents	Contraction coefficients			
1570.277	0.000 017	0.000 031	−0.000 198	0.000 299
373.304 0	0.000 147	0.000 303	−0.002 063	0.003 352
121.962 8	0.000 834	0.001 843	−0.016 256	0.030 007
46.960 09	0.003 581	0.009 829	−0.103 669	0.198 226
19.993 23	0.012 224	0.030 824	−0.288 302	0.450 015
9.076 143	0.034 785	0.067 408	−0.328 447	0.264 082
4.318 022	0.085 626	0.126 952	−0.301 810	−0.275 781
2.133 179	0.174 836	0.378 076	−0.162 552	−1.072 763
1.076 317	0.276 295	0.464 986	0.673 576	0.500 434
0.545 664	0.322 268	−0.229 548	0.396 569	1.068 722
0.275 678	0.238 135	−0.592 062	−0.438 053	−0.536 290
0.137 926	0.070 782	−0.225 622	−0.262 879	−0.394 812
0.066 745	0.002 775	−0.008 157	−0.011 237	−0.022 140

Table 3. The four contracted hydrogen s orbitals.

Exponents	Contraction coefficients			
51.79	0.002 79	−0.000 04	0.002 52	0.001 49
16.89	0.005 83	−0.003 49	−0.005 62	−0.028 79
6.089	0.022 27	0.006 85	0.043 22	0.080 22
2.368	0.064 95	−0.046 92	−0.090 27	−0.419 87
0.975	0.142 92	0.084 03	0.413 83	0.990 90
0.412	0.358 62	−0.320 06	−0.730 79	−3.630 90
0.151 24	0.437 18	0.715 40	3.503 00	6.098 42
0.07	0.095 03	−2.058 70	−5.194 97	−4.543 92
0.03	0.015 76	2.200 30	2.137 98	1.318 27

The atomic basis is presented in tables 1–4. It consists of 66 contracted Gaussian-type orbitals (GTOs), formed from a larger basis of 105 GTOs (Partridge 1989), including d functions on nitrogen, and p functions on hydrogen to account for angular correlation and polarization effects. Some atomic natural orbitals (ANO) were employed for the contractions (Almlof *et al* 1988), although the different electronic configurations of the various states

Table 4. The three hydrogen contracted p_x, p_y and p_z orbitals.

Exponents	Contraction coefficients		
8.9	0.000 37	0.000 41	−0.002 30
2.12	0.003 17	−0.006 73	0.009 95
0.667	0.020 27	0.016 00	−0.111 73
0.231	0.098 72	−0.171 17	0.206 51
0.088 8	0.307 42	0.296 72	−2.146 83
0.037 222	0.491 00	−1.633 09	2.772 87
0.016 151	0.238 15	1.796 03	−1.115 54

considered prevented the use of a pure ANO basis.

When generating the CI wavefunctions, all single and double excitations from a reference space were generated. This reference space comprized all configurations contributing more than $c^2 = 0.01$ at any internuclear separation. To limit the size of the calculation, the 1s orbitals of N were frozen and only configurations that contributed more than 10^{-7} E_h to the energy lowering were included in the CI space (1 $E_h \equiv 27.21$ eV). The typical number of configurations employed ranged between 2000 and 16 000, depending on the molecular symmetry and the internuclear distance.

As noted by Bell *et al* (1992) in their calculations of oscillator strengths in N^+, the choice of both the orbitals and the reference configurations is complicated by the difference in the s and p occupancies for the s^2p^2 and sp^3 configurations and the high correlation in the system. Care has been taken to ensure that the asymptotic energy differences between the entrance channel and the main charge-exchange channels are as accurate as possible, with an error of less than 0.01 E_h.

The adiabatic energies for $(NH)^{2+}$ triplet states are shown in figures 1(*a*) and (*b*) for states of even and odd symmetry, respectively. The molecular symmetry designations of the entrance channels and the possible exothermic channels for charge transfer, along with their calculated exothermicities are:

$N^{2+}(1s^22s^22p\ ^2P^o) + H(1s)$	0.0	$3^3\Pi,\ 2^3\Sigma^+$
$N^+(1s^22s2p^3\ ^3P^o) + H^+$	2.18 eV	$2^3\Pi,\ 1^3\Sigma^+$
$N^+(1s^22s2p^3\ ^3D^o) + H^+$	4.81 eV	$1^3\Pi,\ 1^3\Sigma^-,\ 1^3\Delta$
$N^+(1s^22s^22p^2\ ^3P) + H^+$	15.80 eV	$^3\Pi,\ ^3\Sigma^-$.

The lowest-lying channel is effectively uncoupled from the others due to the large energy difference and has not been included in the dynamical calculations. Accordingly we have numbered the molecular states starting from those that dissociate to $N^+(2s2p^3\ ^3D^o) + H^+$.

To assess the accuracy of our wavefunctions, we have calculated the atomic oscillator strengths of two optically allowed transitions in N^+ using wavefunctions in the asymptotic limit, $R \to \infty$, where R is the internuclear separation. A comparison with the computed values of Bell *et al* (1992) and with other theoretical and experimental results is made in table 5. Our results agree within 3% with recent atomic calculations, suggesting that our description of correlation in N^+ is adequate.

The entrance channel has an attractive polarization interaction at large internuclear distances and its potential energy varies approximately as $-9/R^4$ for $R > 5.5\ a_0$. At small separations, the energy increases exponentially owing to exchange forces, leading to a minimum at $R \simeq 5\ a_0$ of depth $0.007E_h$. The charge-transfer channels generally present a repulsive ion–ion interaction and their energies behave as $+1/R$ for $R > 3\ a_0$, apart from the pseudocrossing regions.

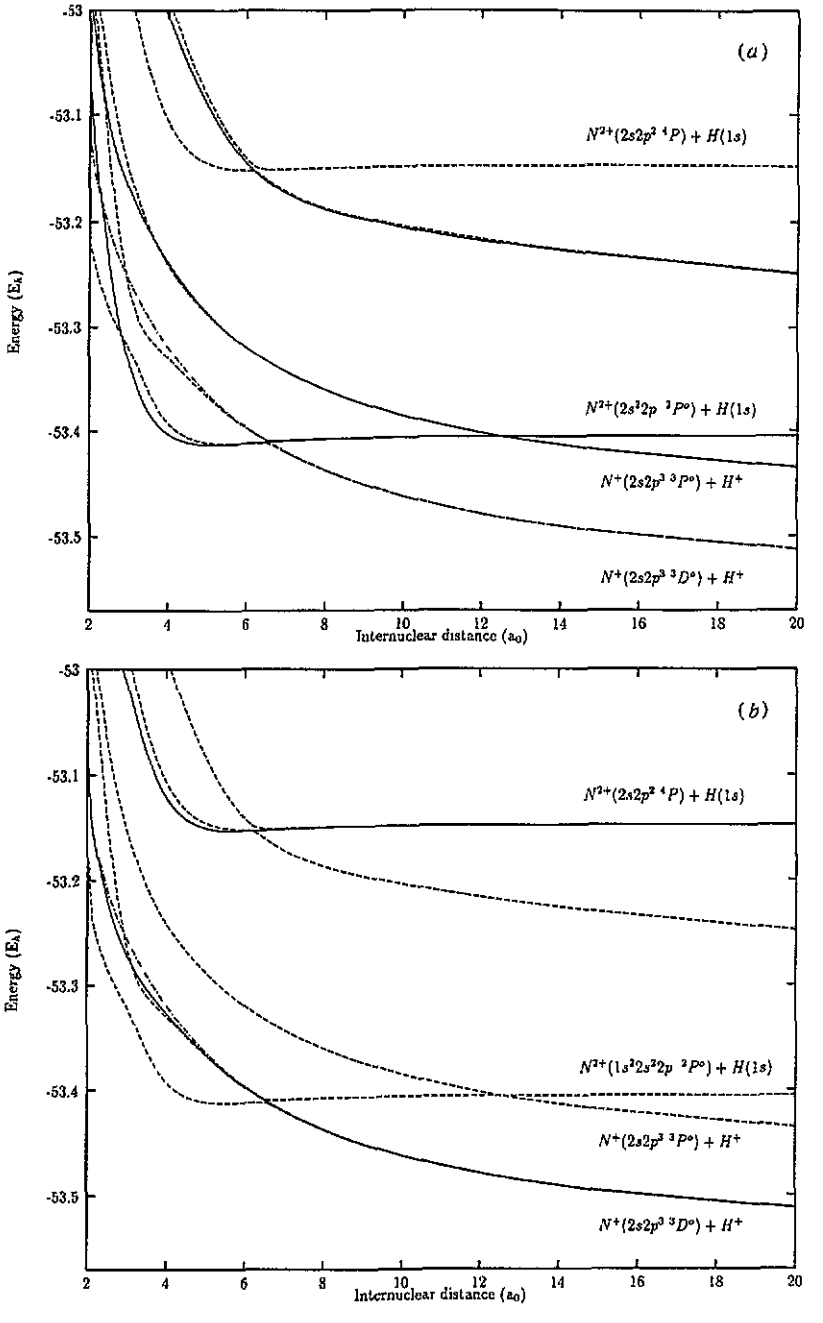

Figure 1. Adiabatic electronic energies for the triplet states of the $(NH)^{2+}$ quasimolecule, as functions of the internuclear distance R. (——): $^3\Sigma$-symmetry molecular states. (- - - -): $^3\Pi$-symmetry molecular states. (— · —): $^3\Delta$-symmetry molecular states. (*a*) Even symmetry. (*b*) Odd symmetry.

In the corresponding singlet system, shown in figure 2, the charge-exchange channels are at higher energies than those of the triplets dissociating to the same configuration.

Table 5. Oscillator strengths in N^+.

Transition	f^a	f^b	f^c						
$(2s^22p^2\ ^3P) \rightarrow (2s2p^3\ ^3D^o)$	0.109	0.112	0.237[d]	0.097[e]	0.101[f]	0.117[g]	0.198[h]	0.134[i]	0.108[j]
$(2s^22p^2\ ^3P) \rightarrow (2s2p^3\ ^3P^o)$	0.163	0.164	0.171[d]	0.133[e]	0.172[f]	0.223[g]	0.191[h]	0.216[i]	0.162[j]

[a] Present results.
[b] Bell *et al* (1992).
[c] Other theoretical results.
[d] Kelly (1964).
[e] *Sinanoglu (1973) and Nicolaides (1973).*
[f] Mallow and Bagus (1976).
[g] Mitroy *et al* (1979).
[g] Ganas (1979).
[h] Fawcett (1987).
[i] Luo and Pradhan (1989).

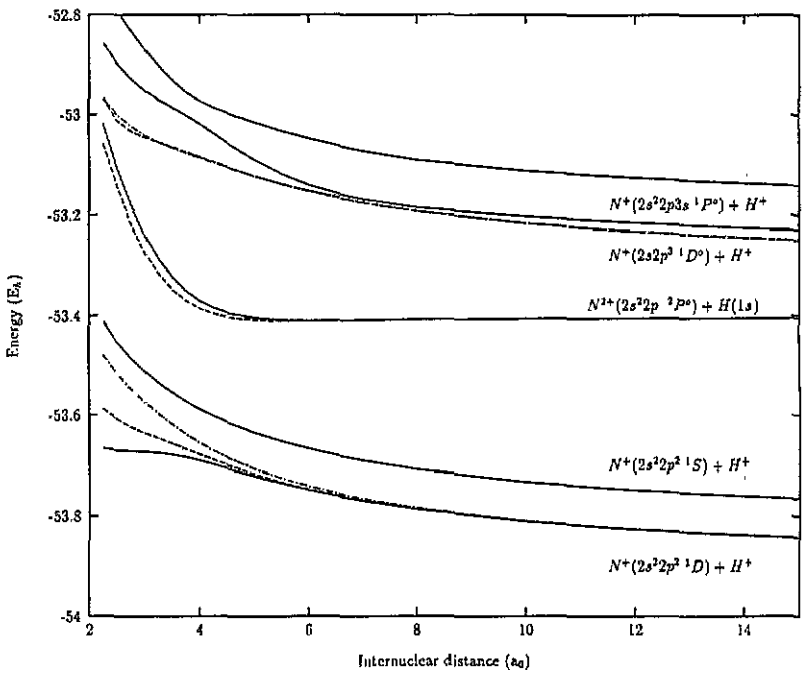

Figure 2. Adiabatic electronic energies for the singlet states of the $(NH)^{2+}$ quasimolecule, as functions of the internuclear distance R. (——): $^1\Sigma^+$-symmetry molecular states. (- - - -): $^1\Pi$-symmetry molecular states. (— · —): $^1\Delta$-symmetry molecular states.

The lowest singlet term arising from the $2s2p^3$ configuration is now endothermic and even the highest term, ^1S, arising from the ground $2s^22p^2$ configuration of N^+ does not show a pseudocrossing with the entrance channel (EC). Hence, collision processes involving the singlet system are not expected to contribute to charge transfer (CT) in the energy range relevant here and the corresponding cross section is taken to be zero.

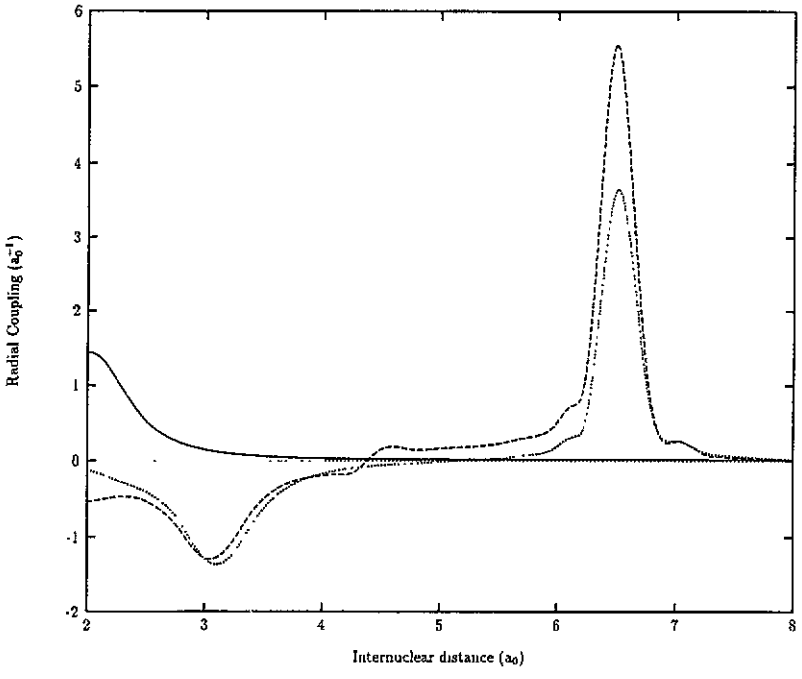

Figure 3. Radial couplings. (——): $2\,^3\Pi - 3\,^3\Pi$ radial coupling. (· · · · · ·): $1\,^3\Pi - 2\,^3\Pi$ radial coupling. For comparison, the result of a Hellmann–Feynman calculation of the $1\,^3\Pi - 2^3\Pi$ radial coupling is also shown (- - - -).

2.2. *Non-adiabatic couplings*

Radial couplings have been calculated using a finite-difference method as described by Forster *et al* (1991). Both rotational couplings and the corrections due to the inclusion of a common translation factor (Errea *et al* 1982, Gargaud *et al* 1987) have been calculated analytically.

The main radial coupling, involving the EC and the channel dissociating to $N^+(^3D^o)+H^+$ in $^3\Pi^-$ symmetry, is shown in figure 3, including the corrections due to the translation factors, although those are negligible in this case. We have also displayed for comparison the Hellmann–Feynman result calculated at the mid-point of the nuclei. There are two peaks in the magnitude of the coupling, centred on the positions of the corresponding pseudocrossings. The outer one, at $R \simeq 6.5\ a_0$, occurs at an essentially ionic–covalent pseudocrossing. The adiabatic energy difference and non-adiabatic coupling can be fitted to the Landau–Zener (LZ) model, with the diabatic coupling $H_{12} = 0.001\,45\ E_h$, the difference in slope $|\Delta F| = 0.026$ au and $R_0 = 6.545\ a_0$. It should be noted that, for this radial coupling, the contribution from the change in the CI coefficients dominates that from the changes in the molecular orbitals over a wide range of internuclear distances in the vicinity of the peak (Cooper 1991). Although this is the most important pseudocrossing, insufficient information is given by Heil *et al* (1981) to allow a detailed quantitative comparison between the two calculations. However, the maximum value of the coupling is similar in the two calculations.

At the inner avoided crossing, near $R = 2.9\ a_0$, both potential curves are rising exponentially as the internuclear separation decreases (see figure 1(*b*)), and neither

the Landau–Zener nor the exponential model (Nikitin and Umanskii 1984) provides a satisfactory parametrization of the numerical results.

The coupling between the EC and the $2\,^3\Pi$ channel, which dissociates into $N^+(2s2p^3\ ^3P^o)$, has a peak centred at $R \simeq 12.5\ a_0$ which is Lorentzian in shape. The area under the peak is $\simeq \pi/2$, and the crossing is traversed diabatically in the energy range of interest here. Our value of the diabatic coupling at the crossing is $H_{12} = 2 \times 10^{-5}\ E_h$, while Butler and Dalgarno (1980) estimated $6 \times 10^{-6}\ E_h$ for this two-electron process. A more important pseudocrossing of these two states occurs at $R \simeq 2.2\ a_0$ (see figure 1(*b*)), where the corresponding coupling, also shown in figure 3, displays a peak that falls off slowly at increasing values of R.

The rotational couplings remain close to their asymptotic value of 1 for channels dissociating to the same limit until the $\Sigma - \Pi - \Delta$ degeneracy is broken by the crossing of the Σ^+ and Σ^- curves at about $6.5\ a_0$.

3. Cross sections

To facilitate the quantal scattering calculation the radial couplings have been transformed to a diabatic representation in the standard way (Smith 1969). In our calculation the two-state diabatic transformation parameter (as used by Heil *et al*) for the $1\,^3\Pi^-$–$2\,^3\Pi^-$ coupling increases smoothly to $\pi/2$ as R decreases through the pseudocrossing region at $R \simeq 6.5\ a_0$, while that of Heil *et al* shows a maximum of about 1.4. The resulting set of coupled equations has been solved using the QUANTXS code (Allan 1991).

The total cross section has been determined as a weighted average according to the statistical ratio 1 : 3 for the probability of singlet and triplet scattering in the entrance channel; we have taken the singlet contribution to be zero in the energy range of interest here.

Within the triplet coupled equations, the calculation can be split into two parts associated with even and odd symmetry with respect to reflection in a plane containing the molecular axis. As the behaviour differs significantly in the two symmetries, we discuss our results separately for each case. The triplet cross section has been calculated as an average of the three contributions, namely $^3\Pi^-$, $^3\Sigma^+$ and $^3\Pi^+$. We have assumed that the values of Heil *et al* and Bienstock *et al* have been determined with equal contributions from $^3\Pi^+$ and $^3\Pi^-$ and zero contribution from $^3\Sigma^+$.

3.1. Odd symmetry

The dynamics of the collision for the odd symmetry follow a simple pattern in the low-energy region ($E \leqslant 10$ eV amu^{-1}). The pseudocrossing of the EC with the channel that dissociates to the atomic state $N^+(^3P^o)$ is diabatically traversed in this energy range, due to the very small energy splitting at the pseudocrossing, as discussed above. Hence, for $6.5\ a_0 \leqslant R \leqslant 12.5\ a_0$ the $2\,^3\Pi^-$ channel retains the character of the EC.

The main contribution to the charge transfer cross section comes from transitions at the pseudocrossing around $R \simeq 6.5\ a_0$ between the $2\,^3\Pi^-$ channel and the $1\,^3\Pi^-$ channel. While there are no states of odd symmetry asymptotically degenerate with the $2\,^3\Pi^-$ channel, and therefore no strong rotational couplings in the EC, the population following the transition is distributed via rotational couplings to the $1\,^3\Sigma^-$ and $1\,^3\Delta^-$ channels that are asymptotically degenerate with $1\,^3\Pi^-$. As shown in figure 4, for an impact energy of $E = 0.92$ eV amu^{-1}, the sum of the $|S_L|^2$ matrix elements, where S is the scattering matrix and L the orbital angular momentum quantum number, from the entrance channel

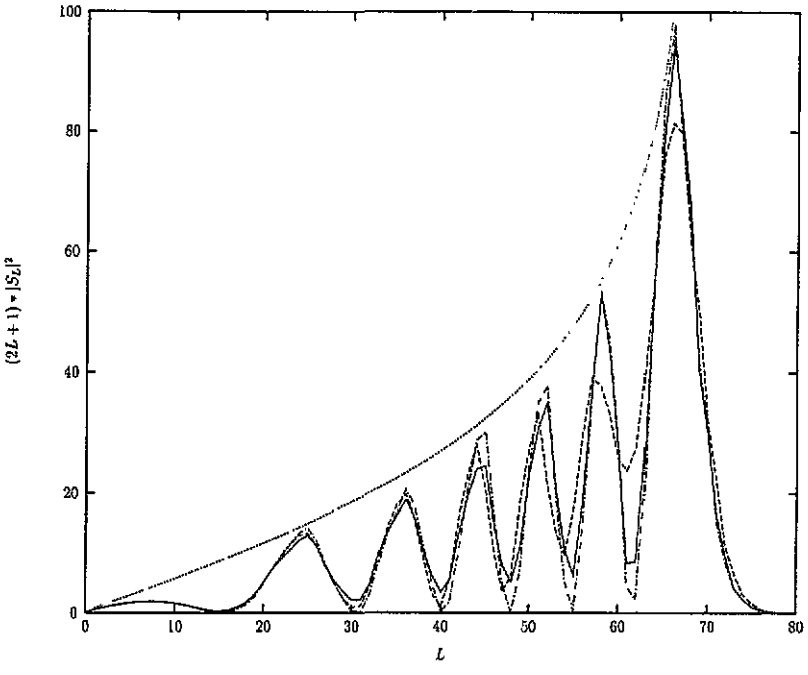

Figure 4. $(2L + 1) * |S_L|^2$ matrix elements for $E = 0.92$ eV amu^{-1}. (——): EC $\rightarrow$ $1\Pi^- + 1\Sigma^- + 1\Delta^-$. (- - - -): EC $\rightarrow$ $1\Pi^+ + 1\Delta^+$. (· · · · · ·): EC $\rightarrow$ 1Π using the Landau–Zener model. (— · —): results from a two-state calculation.

to these three channels is approximately equal to that for a Π channel in a two-state calculation. The sum can be quite accurately reproduced with the semiclassical quantity $\mathcal{P}_{12}$ of the Landau–Zener model (Nikitin and Umanskii 1984) using the parameters obtained in section 2.2. For clarity in the figure we have taken $\sin^2\phi = 1$, in the notation of Nikitin and Umanskii (1984), so that only the maxima should be compared with the LZ results.

The transition probabilities from the EC to the $2^3\Pi^-$ and the $1^3\Pi^-$ channel display the same L-dependence; this is consistent with a two-stage mechanism, involving first the primary radial coupling at $R \simeq 6.5\ a_0$ of the EC with the $1^3\Pi^-$ channel, followed by a secondary radial coupling between the $1^3\Pi^-$ and the $2^3\Pi^-$ channels. This coupling decreases very slowly with internuclear distance, and the integration has been taken to $R = 35\ a_0$.

For energies up to $\simeq 8$ eV amu^{-1}, the cross section obtained from the present calculation differs by less than 5% from that obtained from a two-state calculation including only radial couplings between the EC and the $1^3\Pi^-$ channel and differs by less than 15% from the LZ result using the parameters listed in section 2.2 for energies between 0.25 eV amu^{-1} and 10 eV amu^{-1}. At low energies, $E \leqslant 0.5$ eV amu^{-1}, quantal effects become increasingly important and the semiclassical Landau–Zener model does not reproduce the calculated cross sections and transition probabilities.

When the energy exceeds 10 eV amu^{-1}, significant contributions to the transition probabilities occur at the innermost pseudocrossing near $R_0 = 2.9\ a_0$ between the $1^3\Pi^-$ channel and the EC. For $L \leqslant kR_0$, where k is the wavenumber, the corresponding $|S_L|^2$ matrix elements are determined by this crossing. Figure 5 shows, for an energy

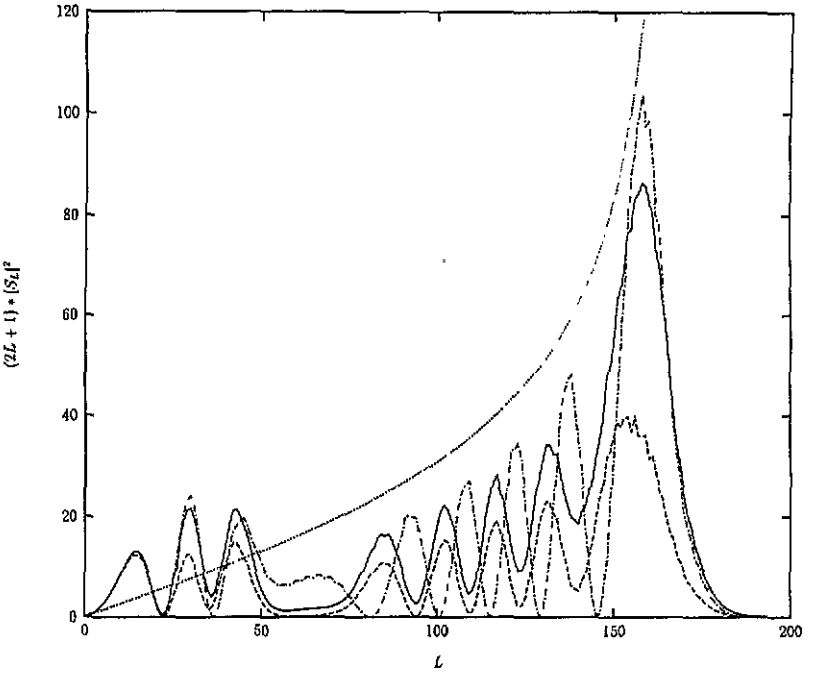

Figure 5. $(2L + 1)|S_L|^2$ matrix elements for $E = 5.34$ eV amu^{-1}. (——): EC $\rightarrow$ $1\Pi^- + 1\Sigma^- + 1\Delta^-$. (- - -): EC $\rightarrow$ $1\Pi^-$. (·····): EC $\rightarrow$ $1\Pi^-$ *using the Landau–Zener* model. (— · —): results from a two-state calculation.

$E = 5.34$ eV amu^{-1}, that the Landau–Zener model overestimates the transition probability. This overestimate is, fortuitously, compensated by the additional contributions from the transitions at the inner pseudocrossing: at such energies, the ^{3}P^o state is populated directly from the EC via the radial coupling near $R = 2.2\ a_0$ between the $2^3\Pi^-$ and $3^3\Pi^-$ channels. In this energy range, the cross section for the production of $N^+(2s2p^3\ ^3P^o)$ is comparable with that for the ^{3}D^o state; rotational couplings between non-degenerate states also become important in populating the ^{3}D^o state.

3.2. Even symmetry

Here there are entrance channels with both $^3\Sigma^+$ and $^3\Pi^+$ symmetry. However, the primary pseudocrossing around $R \simeq 6.5\ a_0$ involves only the $^3\Pi^+$ channel as the $^3\Sigma$ channel dissociating to $H^+ + N^+(2s\,2p^3\ ^3D^o)$ has $^3\Sigma^-$ symmetry (see figures 1(*a*), (*b*)). One expects that, for energies below 10 eV amu^{-1}, where the pseudocrossings near $R \simeq 6.5\ a_0$ are dominant, the $^3\Pi^+$ channel would make a similar contribution to charge transfer as the $^3\Pi^-$. However, there will be no contribution from the $^3\Sigma^+$ entrance channel. Results for $|S_L|^2$, shown in figure 4, confirm this.

Although significant rotational coupling occurs in both the entrance and exit channels, the charge transfer cross section, shown in figure 6, is approximately half its equivalent in the odd symmetry, consistent with the absence of a $^3\Sigma^+$ contribution.

The other mechanisms leading to charge transfer are very similar to those in the odd symmetry.

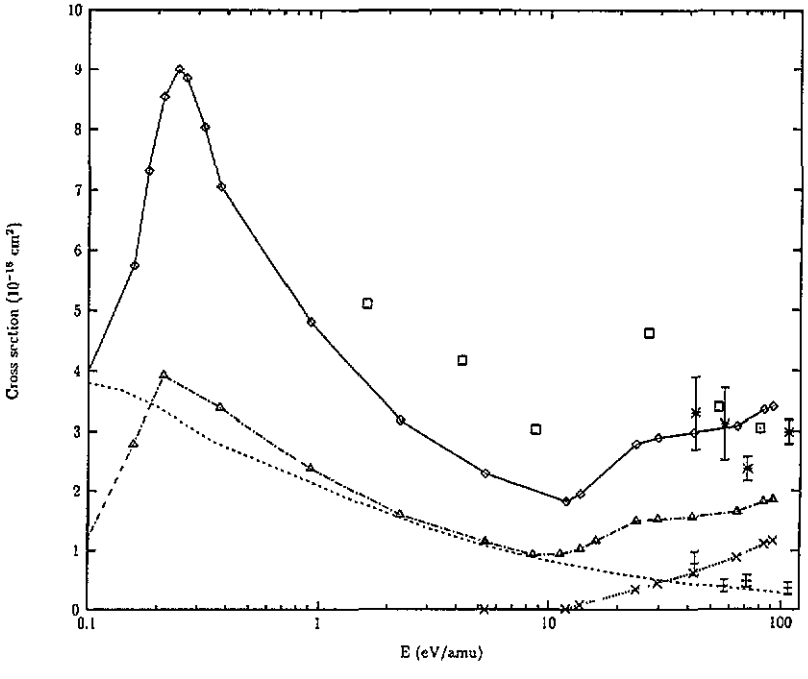

Figure 6. Cross sections for reaction (1). (– ◇ –): total $^3D^o$. (· · · × · · ·): total $^3P^o$. (– · △ – ·): $^3D^o$ contribution from odd symmetry states. (- - - -): Landau–Zener approximation to $^3D^o$. (□): Heil *et al* (1981) and Bienstock *et al* (1986) $^3D^o$. (+): Wilkie *et al* (1985) $^3P^o$. (∗): Wilkie *et al* (1985) $^3D^o$.

3.3. Total charge transfer cross section

The cross sections are presented in figure 6. Our results for the CT cross section from $N^{2+}(^2P^o)$ + H peak at an energy of 0.25 eV amu^{-1}. Below this energy our values are substantially below those of Heil *et al* (1981), which are off the scale of figure 6 as plotted. They considered only radial couplings in $^3\Pi^-$ channels. While quantal interference and resonances are important at these energies, it is clear that the peak of their cross section occurs at a lower energy than is predicted by the present calculations.

For energies between 0.25 and 8 eV amu^{-1} our cross sections are 20–40% smaller than those of Heil *et al* (1981). At 26.8 eV amu^{-1} our results are 40% below those of Bienstock *et al* (1986), but their results and ours cross around 70 eV amu^{-1}.

The differences between our calculation and that of Heil *et al* (1981) for energies less than 8 eV amu^{-1} arise principally, not from the number of channels included in the scattering calculation, but from small variations in the position of the pseudocrossing and, particularly, the potential energy difference there. Owing to the sensitivity to these parameters of the energy at which the maximum of the cross section occurs, small variations can lead to significant differences in the total cross section.

Even though most of the measurements of Wilkie *et al* (1985) are too high in energy to be of interest for the present calculation, the comparison with their results for $N^+(^3D^o)$ production at energies between 43 eV amu^{-1} and about 100 eV amu^{-1} (see figure 6) shows encouraging agreement, although we have not optimized our calculation for this region.

Table 6. Rate coefficients (10^{-9} cm^3 s^{-1}) for reaction (1).

Temperature (K)	Total	$^3D^o$	$^3P^o$
1 000	0.213	0.213	3.4×10^{-7}
1 500	0.319	0.319	6.5×10^{-7}
2 000	0.392	0.392	9.4×10^{-7}
2 500	0.438	0.438	1.3×10^{-6}
3 000	0.467	0.467	1.7×10^{-6}
3 500	0.493	0.493	2.3×10^{-6}
4 000	0.514	0.514	2.9×10^{-6}
4 500	0.530	0.530	3.6×10^{-6}
5 000	0.544	0.544	4.5×10^{-6}
5 500	0.556	0.556	5.4×10^{-6}
6 000	0.566	0.566	6.4×10^{-6}
6 500	0.574	0.575	7.5×10^{-6}
7 000	0.582	0.582	8.8×10^{-6}
7 500	0.589	0.589	1.0×10^{-5}
8 000	0.595	0.595	1.2×10^{-5}
8 500	0.600	0.600	1.4×10^{-5}
9 000	0.605	0.605	1.6×10^{-5}
9 500	0.609	0.609	1.8×10^{-5}
10 000	0.613	0.613	2.1×10^{-5}
15 000	0.642	0.642	8.1×10^{-5}
20 000	0.663	0.663	2.7×10^{-4}
25 000	0.682	0.681	6.8×10^{-4}
30 000	0.700	0.670	1.4×10^{-3}
40 000	0.747	0.743	4.4×10^{-3}
50 000	0.808	0.798	1.0×10^{-2}
60 000	0.881	0.862	1.9×10^{-2}
70 000	0.962	0.932	3.0×10^{-2}
80 000	1.045	1.004	4.2×10^{-2}
90 000	1.132	1.078	5.4×10^{-2}
100 000	1.222	1.154	6.8×10^{-2}

In their work, Bienstock *et al* (1986) examined the production of the $^3P^o$ state through the distant pseudocrossing at $R \simeq 11\ a_0$. They estimated that the maximum of the $^3P^o$ cross section should be at energies well below those investigated by Wilkie *et al*, and concluded that this mechanism was not important. Our investigations of this pseudocrossing confirm their conclusion. However, the additional crossing at small distances, $R \simeq 2.2\ a_0$, which would give a maximum cross section of about 2 Å^2, provides an explanation of the measurements: these show the cross section rising to 1.5 Å^2 at about 570 eV amu^{-1}. Our values for the $^3P^o$ cross section lie above the measurements of Wilkie *et al* between 43 and 100 eV amu^{-1}. However, since the energy range studied by Wilkie *et al* was not our primary concern, we have not investigated this crossing more closely.

Values of the rate coefficient for reaction (1) for temperatures between 10^3 and 10^5 K are shown in figure 7. Our values for 5×10^3–5×10^4 K lie about 30% below those of Heil *et al* (1981), consistent with the differences in the cross sections discussed previously. Using their tabulated cross sections, our rough estimate of the rate coefficient at lower temperatures suggests that our values fall faster as the temperature decreases, consistent with the peak in our cross section occurring at a higher energy than that of Heil *et al*. Table 6 lists the values of the rate coefficient for the $^3P^o$ state. They are considerably smaller than the corresponding values for the $^3D^o$ state, which are also tabulated.

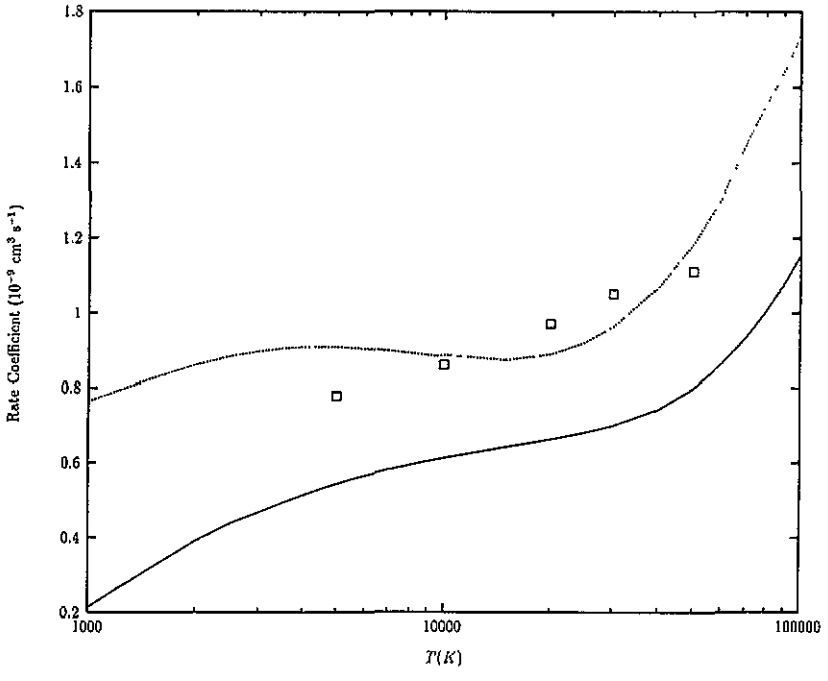

Figure 7. Rate coefficients for reaction (1). (——): capture into $^3D^o$. (· · · · · ·): our estimate of the $^3D^o$ rate coefficient using the cross sections of Bienstock *et al* (1986). (□): Heil *et al* (1981).

4. Rate coefficient

The charge transfer rate coefficient has been calculated as

$$\alpha(T) = \left[\frac{8k_BT}{\pi\mu}\right]^{1/2} \int_0^\infty x\,\sigma\,e^{-x}\,dx$$

where $x = E/k_BT$, k_B is the Boltzmann constant, E is the kinetic energy in the entrance channel, μ the reduced mass and σ is the charge-transfer cross section.

The cross section was evaluated at 17 points to generate a Chebyshev fit over the energy range 0.0092–91.7 eV amu^{-1}. Minor modifications were made to the very small low-energy cross sections ($E < 0.03$ eV amu^{-1}) to ensure a smooth fit in the region where the cross section changes rapidly with energy. The fitted cross section was then integrated using the method of O'Hara and Smith (1970). Results obtained using a nine-point fit differed by less than 3% from those deriving from the full 17-point calculation.

5. Conclusions

We have calculated charge-transfer cross sections using an 11 triplet state molecular expansion of the $(NH)^{2+}$ wavefunction, including an electron translation factor in the dynamical calculations. Singlet states of $(NH)^{2+}$ have been examined and estimated to make a negligible contribution to charge-transfer cross sections at low energies. Our values for the total charge-transfer cross section are 20–40% smaller than the previous two-state results of Heil *et al* (1981) for energies between 0.25 and 27 eV amu^{-1}. At lower energies,

larger discrepancies occur because the energy of their maximum cross section is lower. This difference probably relates to the computed separations of the adiabatic potential energy curves in the region of the principal pseudocrossing and the associated non-adiabatic coupling. For energies between 0.5 and 8 eV amu^{-1} the Landau–Zener model yields a satisfactory approximation.

The behaviour of the cross section measured by Wilkie *et al* (1985) above 43 eV amu^{-1} for production of the $^3P^o$ state can be explained qualitatively in terms of transitions at an inner pseudocrossing, not considered in previous calculations.

Charge-transfer rate coefficients have been calculated for temperatures between 10^3 K and 10^5 K. Our results for temperatures between 5×10^3–5×10^4 K lie 28–33% below the earlier calculations of Heil *et al*.

Acknowledgment

This work was supported by a research grant from the UK Particle Physics and Astronomy Research Council (PPARC).

References

Allan R J 1991 Private communication
Almlof J, Helgaker T and Taylor P R 1988 *J. Phys. Chem.* **92** 3029
Almlof J and Taylor P R 1987 *J. Chem. Phys.* **86** 4070
Bates D R and McCarroll R 1958 *Proc. R. Soc.* A **245** 175
Bell K L, Ramsbottom C A and Hibbert A 1992 *J. Phys. B: At. Mol. Opt. Phys.* **25** 1735
Bienstock S, Dalgarno A and Heil T G 1986 *Phys. Rev.* A **33** 2078
Butler S E and Dalgarno A 1980 *Astrophys. J.* **241** 838
Cooper I L 1991 *J. Phys. B: At. Mol. Opt. Phys.* **24** 1517
Errea L F, Mendez L and Riera A 1982 *J. Phys. B: At. Mol. Phys.* **15** 101
Fawcett B C 1987 *At. Data Nucl. Data Tables* **37** 411
Forster C, Cooper I L, Dickinson A S, Flower D R and Méndez L 1991 *J. Phys. B: At. Mol. Opt. Phys.* **24** 3433
Ganas P S 1979 *J. Opt. Soc. Am.* **69** 1140
Gargaud M, McCarroll R and Valiron P 1987 *J. Phys. B: At. Mol. Phys.* **20** 1555
Guest M F, Fantucci P, Harrison R J, Kendrich I, van Lenthe J H, Schoeffel K and Sherwood P 1993 *GAMESS-UK* CFS Ltd
Heil T G, Butler S E and Dalgarno A 1981 *Phys. Rev.* A **23** 1100
Kelly P S 1964 *Astrophys. J.* **140** 1247
Kimura M and Lane N F 1990 *Adv. At. Mol. Opt. Phys.* **26** 79
Luo D and Pradhan A K 1989 *J. Phys. B: At. Mol. Opt. Phys.* **22** 3377
Macias A and Riera A 1982 *Phys. Rep.* **90** 299
Mallow J V and Bagus P S 1976 *J. Quantum. Spectrosc. Radiat. Transfer* **16** 409
Nicolaides C A 1973 *Chem. Phys. Lett.* **21** 242
Nikitin E E and Umanskii S Ya 1984 *Theory of Slow Atomic Collisions* (Berlin: Springer)
O'Hara H and Smith F J 1970 *J. Comput. Phys.* **5** 328
Partridge H 1989 *J. Chem. Phys.* **90** 1043
Reader J, Corliss C H, Wiese W L and Martin G A 1980 *Atomic Transition Probabilities* NSRDS-NBS 68 (Washington, DC: US Govt Printing Office)
Sinanoglu O 1973 *Nucl. Instrum. Methods* **110** 193
Smith F T 1969 *Phys. Rev.* **179** 111
Wilkie F G, Yousif F B, McCullough R W, Geddes J and Gilbody H B 1985 *J. Phys. B: At. Mol. Phys.* **18** 479